Nuclear Instruments and Methods in Physics Research B 269 (2011) 440–443

Contents lists available at ScienceDirect

Nuclear Instruments and Methods in Physics Research B

journal homepage: www.elsevier.com/locate/nimb

Ion beam analysis of partial lithium extraction of $LiMn_2O_4$ by chemical delithiation

E. Andrade [a,*], A. Romero Núñez [b], A. Ibarra Palos [b], J. Cruz [a], M.F. Rocha [c], C. Solis [a], O.G. de Lucio [a], E.P. Zavala [a]

[a] Instituto de Física, Universidad Nacional Autónoma de México, Apartado Postal 20-364, 01000 México, D.F., Mexico
[b] Instituto de Investigaciones en Materiales, Universidad Nacional Autónoma de México, A.P. 70-360, México D.F. 04510, Mexico
[c] ESIME-Z, Instituto Politécnico Nacional, U.P. ALM, G.A. Madero, México D.F. 07738, Mexico

ARTICLE INFO

Article history:
Received 8 October 2010
Received in revised form 9 December 2010
Available online 21 December 2010

Keywords:
$LiMn_2O_4$
Chemical delithiation
XRD
EBS
NRA

ABSTRACT

Lithium manganese oxide, $LiMn_2O_4$, has been studied by many research groups. This material is a great candidate to be used as positive electrode in rechargeable lithium-ion batteries because of its low cost, abundant precursors and non-toxicity. $LiMn_2O_4$ has a spinel Fd-3m structure and shows a reversible extraction and insertion of lithium ions that is one of the most important characteristic of positive electrodes in rechargeable batteries.

In this work, $LiMn_2O_4$ samples were synthesized by solid state reaction. A partial lithium removal was performed on this system by chemical delithiation using HCl aqueous solutions at different concentrations. Six partial-extracted compounds were obtained and characterized by Ion beam analysis (IBA) in order to obtain the Li concentrations. X-ray diffraction (XRD) and Rietveld analyses were also performed. A rigorous study of lithium contents is critical to analyze the structure properties of these compounds and samples production parameters. The IBA method used in this work was the analysis of energy spectra of elastic backscattered (EBS) proton from Mn, O and Li nuclei and the α-particles energy from the $^7Li(p,\alpha)^4He$ nuclear reaction (NR).

1. Introduction

Many actual environmental problems are consequence of the use of non-renewable and fossil-based energy sources. To sustain growing industrial and societal energy demands in an environmentally friendly way, will require the use of clean energy sources such as solar, wind, nuclear, electric batteries, etc. Lithium-ion battery technology offers storage and energy conversion devices with high energy density, power and long life suitable for several new applications like hybrid and electric vehicles [1]. In addition, the lithium-ion battery has become the basis of a huge market for portable devices because it offers smaller sizes and longer runtime than other rechargeable technologies as lead acid and nickel-metal hydride [2]. One of the reasons to use lithium ion is its lightness and its high electropositive potential [2]. It is also a strategic material that can be used in other energy applications such as nuclear fusion. Lithium is widely distributed on Earth; the biggest deposits have been found in Bolivia, Argentina, and more recently, in Mexico.

Basically, a Li-ion cell consists of a positive and negative electrode and an electrolyte between them, which must be ionic conductor and electronic insulator. Once positive and negative electrodes are linked by external connector a spontaneous electrochemical reaction take place, in which chemical energy is transformed into electrical energy [3]. A reverse reaction can proceed under an applied electric current. These reactions are known as discharge and charge processes and involve a diffusion of lithium-ion to the positive electrode: insertion and extractions, respectively. Some characteristics of the batteries, as rate performance, are usually limited by positive electrode and several researches are in progress to develop major capacitive materials [4].

Current lithium-ion positive electrode material mostly consists of $LiCoO_2$ that has high cost and toxicity. One attractive material to be used as positive electrode is the $LiMn_2O_4$ spinel, with an Fd-3m space group, that has lower cost and toxicity compared to $LiCoO_2$. To obtain $LiMn_2O_4$ spinel with excellent electrochemical characteristics, several techniques, such as sol–gel, melt-impregnation and solid-state process [5–7] have been developed. Although these methods improve the electrochemical properties of spinel, to some extent, there are still some problems, such a phase transition near to the room temperature and difficult operation or scale-up. The consequence of the phase transition is a fading in the capacity, due to the presence of an undesirable impure phase, and produces a decrease in delivered energy. Therefore, much research is directed towards synthesizing lithium–manganese spinel oxides with characteristics that can overcome these problems. One way to overcome them is the lithium extraction of the $LiMn_2O_4$. This

* Corresponding author.
E-mail address: andrade@fisica.unam.mx (E. Andrade).

0168-583X/$ - see front matter © 2010 Elsevier B.V. All rights reserved.
doi:10.1016/j.nimb.2010.12.036

extraction can be performed by two methods: electrochemical and chemical. The last one consists in an acid treatment, usually hydrochloric or sulfuric acid. This kind of extraction maintains the Mn_2O_4 framework structure [8] and diminishes that capacitive-loss effect [9].

In this work we investigated $LiMn_2O_4$ samples with chemical lithium extraction performed using different hydrochloric acid concentrations to study the changes in the crystal structure. This process is known as chemical delithiation [10]. The determination of lithium concentrations is crucial to evaluate the sample preparation method and to analyze change in the crystal structure properties of these compounds.

It is known that conventional material analysis methods such as laser induced breakdown spectroscopy, atomic, absorption, etc., have poor sensitivity to measure the Li concentration in solid, because of its low atomic number.

Direct, nondestructive and absolute measurements of Li concentration in solids can be carried out by different ion beam analysis (IBA) methods. High energy accelerators using heavy ions can be used to measure the energy recoil of the lithium nuclei. This IBA technique is known as energy recoil detection analysis (ERDA) and it is perhaps the best suited IBA method for this study [11]. Low energy particle accelerators ($E \leqslant 10$ MeV) have been used for the quantification of Li [12] through the induced gamma-ray emission (PIGE) through the $^7Li(p,\gamma)^8Be^*$ nuclear reaction analysis (NR).

In this work, a low energy proton beam has been used to measure the atomic concentration profiles of the Mn, O and Li in the samples. The method consists on measuring, in the same energy spectrum, the elastic backscattered (EBS) protons from Mn, O and Li and the α-particles energies from the $^7Li(p,\alpha)^4He$ nuclear reaction (NR).

2. Experimental procedure

2.1. Sample preparation

$LiMn_2O_4$ was prepared by solid state reaction, where a mechanical mixture of Li_2CO_3 (99%, Aldrich) and $MnCO_3$ (99.9%, Aldrich) was annealed at 850 °C for 18 h in air. To obtain partial extracted samples, an acid treatment was carried out by stirring 0.72 g of $LiMn_2O_4$ powder with 100 ml of HCl solution for 18 h; all reactions were followed by conductimetry. Six starting acid concentrations: 2, 4, 7, 9, 12 and 15 mM were used. Finally the samples were washed with deionized water and vacuum dried.

2.2. Ion beam analysis

The Universidad Nacional Autónoma de México Van de Graaff 5.5 MV CN HVECO accelerator was used for the ion beam analysis of the samples. Pellets (8 mm in diameter and 2 mm thick) prepared by compression of the fine powder were bombarded with a proton beam. A surface barrier detector (30 keV FWHM energy resolution) was set at 150° to measure the particle's energy spectra. We did not used an absorbing film in front of the detector, in order to register in the same energy spectrum the elastic backscattered (EBS) protons from the Li, O and Mn nuclei and the α particles from the $^7Li(p,\alpha)^4He$ nuclear reaction (NR).

2.3. XRD analysis

The crystal structure of all samples was obtained by conventional XRD power diffraction analysis using a Brucker D8 Advance diffractometer with Cu Kα ($\lambda = 0.154$ nm) radiation and with a Vantec detector. XRD data were analyzed using the Rietveld refinement with Fulproof program [13].

3. Results and discussion

Fig. 1 shows a typical experimental (dots) spectrum of sample B (see Table 1), bombarded with 1800 keV proton beam. The spectrum has been divided in two parts: (a) a low energy region, that corresponds to the energies of the elastically backscattered (EBS) protons form the Mn, O and Li nuclei, and (b) a high energy region (NR), that corresponds to the energies of the α particles from $^7Li(p,\alpha)^4He$. The EBS and NR regions in the spectrum are well separated, since the $^7Li(p,\alpha)^4He$ NR has a large positive Q-value (14.470 MeV). Kinematic calculations show that α particle from the sample's surface has energy of 7740 keV, compared to 1580 keV for EBS protons from the Mn nuclei.

The solid line in the spectrum represents the SIMNRA [14] simulation of the spectrum. In the simulation we used the $^7Li(p,\alpha)^4He$ NR cross section, non-Rutherford elastic cross sections for O and Li, and Rutherford cross section for Mn. The non-Rutherford cross sections were obtained from the Ion beam analysis nuclear data (IBANDL). SRIM version 2008.03 stopping powers were used to estimate the sample depth probed as 12.4 μm by our proton beam. We used a uniform concentration with depth of all the constituent elements for the SIMNRA [14] simulation for all the samples. The α counting yield is low because $^7Li(p,\alpha)^4He$ NR has a small cross sections compared to the EBS cross sections from Mn and O. However, the α spectrum is background free because there are no other NR particles interfering with the α spectrum. Although the Li concentration is constant with depth, the α particle yield decreases as the proton lose energy in the sample, following the shape of the $^7Li(p,\alpha)^4He$ cross section energy function of the proton energy function.

It may be observed in the SIMNRA simulation of the spectrum that Li EBS counting yield contribution to the spectrum is negligible and masked by the larger number of events from proton scattering off heavier elements deeper in the sample. This is due to the small proton Li cross sections, compared to the other nuclei in the sample. If the SIMNRA simulation is only performed on the EBS region of the spectrum it will give ambiguous Li concentrations. Lithium contribution to the EBS proton spectrum is so small that an acceptable simulation of the EBS spectrum can be obtained without Li. This ambiguity is eliminated by the simultaneous SIMNRA simulation of the EBS and the $^7Li(p,\alpha)^4He$ NR regions.

Table 1 summarizes the results of the IBA of the samples. The unit cell parameters deduced from the XRD pattern analysis are

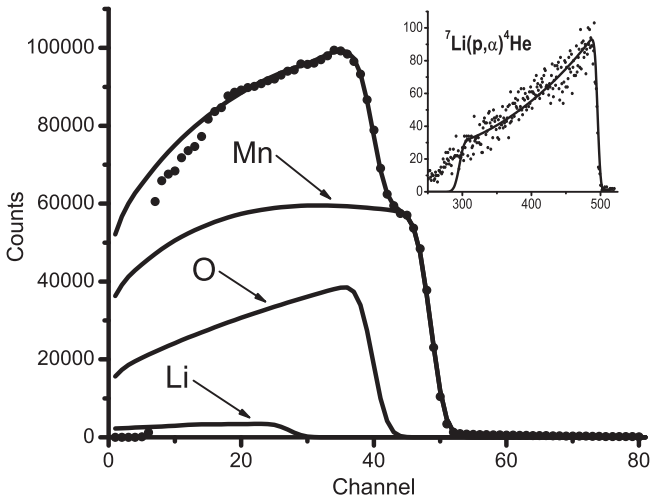

Fig. 1. Experimental spectrum of sample B bombarded with a 1800 keV proton beam. The elastic energies of the backscattered (EBS) protons from Mn, O and the high energies α's particles from the $^7Li(p,\alpha)^4He$ nuclear reaction(NR) are shown separately. The solid line represents the SIMNRA simulation of the spectrum.

Table 1
Summary of the IBA results of $LiMn_2O_4$ partial lithium removed samples. The concentration of HCl used in the chemical delithiation of each sample is given in column 2. The unit cell lattice parameter deduced from the XRD patterns by Rietveld method are also shown in the last column. The error in the elemental concentrations is estimated to be 10%.

Sample	HCl Conc. (mM)	%Li	%O	O/Mn	Cell parameter (Å)
A	0	14	60	2.2	8.2295(2)
B	2	13	56	2.1	8.1998(2)
C	4	12	60	2.2	8.1603(2)
D	7	5.0	65	2.2	8.0639(3)
E	9	3.9	61	1.8	8.0554(2)
F	12	4.0	62	2.0	8.0530(1)
G	15	3.6	64	2.0	8.0546(2)

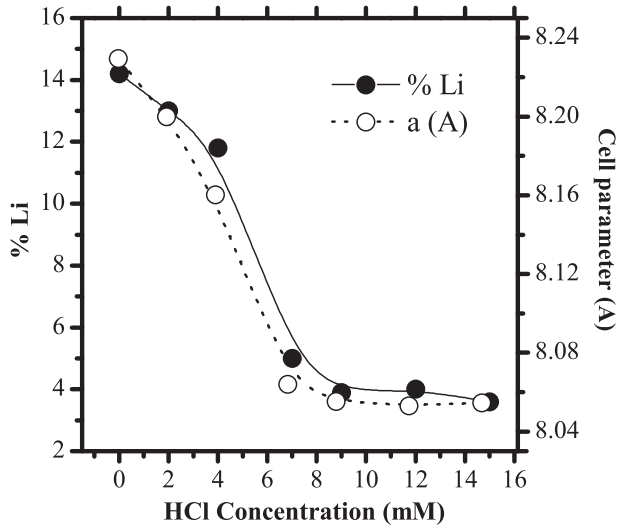

Fig. 2. Lithium percentage content and cell parameter of A–G samples as a function of acid-treatment concentration.

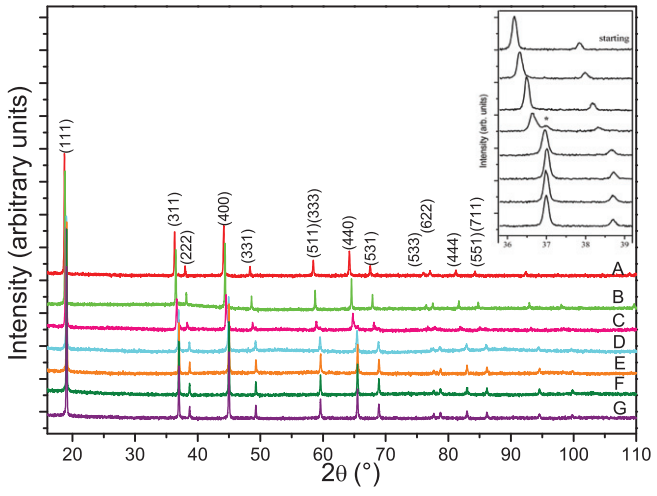

Fig. 3. XRD diffraction patterns of $LiMn_2O_4$ partial lithium removed samples performed by chemical delithiation using HCl aqueous solutions at different concentrations. The inset figure shows a close view of the area of (3 1 1) and (2 2 2) peaks.

shown in the last column. It may observe a decrease in the lithium concentration as the hydrochloric acid concentration increases, while the ratio O/Mn ≈ 2 is maintained for all the samples. These results are also shown graphically in Fig. 2. This tendency is associated with the Li-ion extraction of the housing Mn–O framework structure, confirmed by XRD results as discussed latter.

Fig. 3 shows XRD diffraction patterns of $LiMn_2O_4$ (starting sample A) and six acid-treated samples (B–G). Sample A shows a pure crystal phase identified with spinel $LiMn_2O_4$ structure, indexed in cubic Fd-3m space group. The fact that main diffraction peaks such as (1 1 1), (3 1 1) and (4 0 0) were well developed means that lithium ions occupied tetrahedral 8a sites and manganese also occupied octahedral 16d sites [13]. Lattice parameter obtained by Rietveld analysis was 8.2295 Å. This value is lower than the reported JCPDS value of 8.2480 Å indicating that the sample does not have stoichiometric spinel $LiMn_2O_4$. An explanation for this discrepancy is that the lattice parameter depends on several conditions, such as annealing time, precursors, and manganese oxidation state and lithium contents [6]. Smaller values of the lattice parameter can be due by a decrease of Mn^{3+}/Mn^{4+} ratio by way of keeping more Mn^{4+} than Mn^{3+}.

The XRD patterns of samples B–G are in good agreement with the $LiMn_2O_4$ reported pattern, i.e., number of peaks, and their relative intensities were almost the same as starting sample. The fact that starting sample and acid-treated samples have similar XRD patterns means that $LiMn_2O_4$ framework was preserved after Li^+ ions extraction. Since X-rays are diffracted by electrons on each atom, this technique hardly detects atoms with small atomic number such Li. For that reason lithium ion does not have a significant contribution to the XRD diffraction pattern. Therefore, the Mn and O atoms make the most important contributions to the XRD patterns.

The inset in the same Fig. 3 shows a close view of the area of (3 1 1) and (2 2 2) peaks. The XRD patterns show that the Li extraction produces a slight displacement of the peaks to larger angles. This behavior was caused by the contraction of the unit cell which is the direct consequence of Li-ions extraction and Mn^{3+}oxidation, both phenomena occurring with chemical delithiation [13].

4. Conclusions

An IBA method was used to measure simultaneously the Li, O and Mn content on six $Li_{(1-x)}Mn_2O_4$ samples treated with different hydrochloric acid concentrations. These results show, as expected, that the Li contents on the samples decrease as the hydrochloric acid concentration increases. IBA provides very useful information about sample preparation, i.e., the chemical acid HCl concentrations needed to obtain the Li removal required (see Fig. 2).

The Rietveld refinement analysis of the XRD spectra shows a small decrease in the cell parameter as acid treatment concentration increases, that is also an evidence of Li extraction. These results are consistent with the IBA results.

Electrochemical properties of the partial Li extracted samples are in progress to evaluate the potential use of the $Li_{(1-x)}Mn_2O_4$ as a positive electrode in rechargeable lithium ion batteries.

Acknowledgements

The authors wish to thank Arcadio Huerta for his technical support. We acknowledge the financial support from UNAM-DGAPA-PAPIIT under contracts IN227807; IN219609 and IN105510. Partial financial support from CONACyT CB-2005-01-48883 is greatly appreciated.

References

[1] K. Ozawa, Lithium Ion Rechargeable Batteries, WILEY-VCH, Weinheim, 2009. p. 1.
[2] F. Béguin, E. Frackowiak, Carbons for Electrochemical Energy Storage and Conversion Systems, CRC Press Taylor & Francis Group, New York, 2010. p. 2.
[3] J.M. Tarascon, M. Armand, Nature 414 (2001) 359.

[4] R. Decher, Direct Energy Conversion, Oxford University Press, New York, 1997. p. 162.
[5] Y. Talyosef, J. Electrochem. Soc. 154 (2007) A682.
[6] Yi Ting-Feng, Hao Chun-Li, Yue Cai-Bo, Zhu Rong-Sun, Shu Jie, Synth. Mater. 159 (2009) 1255.
[7] Myung Seung-Taek, Chung Hoon-Taek, Komaba Shinichi, Kumagai Naoaki, Gu Hal-Bon, J. Power Sources 90 (2000) 103.
[8] C. Hunter, Solid State chem. 39 (1981) 142.
[9] J. Molenda, W. Ojczyk, M. Marzec, J. Marzec, J. Przewoźnik, R. Dziembaj, M. Molenda, Solid State Ionics 157 (2003) 73.
[10] S. Venkatraman, A. Manthiram, J. Solid State Chem. 177 (2004) 4244.
[11] A. Climent-Font, M. Cervera, M.J. Hernandez, A. Munoz-Martın, J. Piqueras, Nucl. Instrum. Methods Phys. Res. B 260 (2008) 1498–1501.
[12] R. Mateus, A.P. Jesus, M. Fonseca, H. Luis, J.P. Ribeiro, Nucl. Instrum. Methods Phys. Res. B 264 (2007) 340–344.
[13] Rodríguez-Carbajal, Phys. B 192 (1993) 55.
[14] M. Mayer, SIMNRA User Guide Technical Report IPP 9/113 Max Plank Institut Fur Plamsmaphysik, Garching Germany.